Submodular Variational Inference for Network Reconstruction

Lin Chen[1,2], **Forrest W Crawford**[2,3] and **Amin Karbasi**[1,2]
[1]Department of Electrical Engineering, [2]Yale Institute for Network Science, [3]Department of Biostatistics,
Yale University
{lin.chen,forrest.crawford,amin.karbasi}@yale.edu

Abstract

In real-world and online social networks, individuals receive and transmit information in real time. Cascading information transmissions (e.g. phone calls, text messages, social media posts) may be understood as a realization of a diffusion process operating on the network. The process only traverses and thereby reveals a limited portion of the edges. The network reconstruction/inference problem is to estimate the unrevealed connections. Most existing approaches derive a likelihood and attempt to find the network topology maximizing the likelihood, yielding a highly intractable problem. In this paper, we focus on the network reconstruction problem for a broad class of real-world diffusion processes, exemplified by a network diffusion scheme called respondent-driven sampling (RDS). We prove that under realistic and general models of network diffusion, the posterior distribution of an observed RDS realization is a Bayesian log-submodular model. We then propose VINE, a novel, accurate, and computationally efficient variational inference algorithm, for the network reconstruction problem under this model. Crucially, we do not assume any particular probabilistic model for the underlying network. VINE recovers any connected graph with high accuracy as shown by our experimental results on real-life networks.

1 INTRODUCTION

The network reconstruction problem, also known as the network inference problem (Daneshmand et al., 2014; Kramer et al., 2009; Farajtabar et al., 2015; Liben-Nowell and Kleinberg, 2007; Linderman and Adams, 2014; Anandkumar et al., 2011; Kim and Leskovec, 2011), arises naturally in a variety of scenarios and has been the focus of great research interest. In the most general setting, we assume there is an underlying unknown graph structure that represents the connections between network subjects, and that we can only observe single or multiple diffusion processes over the graph. Usually propagation of the diffusion process can only occur over network edges; however, there exist many hidden ties untraversed or unrevealed by the diffusion processes, and the goal is to infer such hidden ties. This network reconstruction problem arises in several empirical topic areas:

Blogosphere. Millions of authors in the worldwide blogosphere write articles every day, each triggering a diffusion process of reposts over the underlying blog network structure. The diffusion process initiated by an article can be represented by a directed tree. The observed data consist of multiple directed trees and it is of great interest to understand the underlying structure of information flow (Gomez-Rodriguez et al., 2014). Following inference of the network, researchers may apply community detection algorithms to, e.g., aggregate and further analyze blog sites of different political views.

Online social networks. Weibo is a Twitter-like microblogging service in China (Gao et al., 2012) where users post microblogs and repost those from other users they follow. An explicit repost chain, which indicates the sequence of users that a post passes through, is attached to each repost on Weibo. Similarly, each post initiates a diffusion process. By observing several realizations of diffusion processes, researchers seek to understand the underlying social and information network structure.

Respondent-driven sampling. Respondent-driven sampling (RDS) is a chain-referral peer recruitment procedure that is widely used in epidemiology for studying hidden and hard-to-reach human populations when ran-

dom sampling is impossible (Heckathorn, 1997). RDS is commonly used in studies of men who have sex with men, homeless people, sex workers, drug users, and other groups at high risk for HIV infection (Woodhouse et al., 1994). An RDS recruitment process is also a diffusion process over an unknown social network structure, and the diffusion tree (who recruited whom) is revealed by the observed process. In addition, when a subject enters the survey, she reports her total number of acquaintances in the population, or graph-theoretically speaking, her degree in the underlying network. Understanding the underlying network structure is a topic of great interest to epidemiologists and sociologists who wish to study the transmission of infectious diseases, and the propagation of health-related behaviors in the networks of high-risk groups (Crawford, 2016). However, in contrast to the aforementioned scenarios where multiple diffusion realizations are available over the same network, in RDS we can only observe a single realization due to limited financial, temporal and human resources to conduct the experiments. As a result, network reconstruction from RDS data is particularly challenging and only heuristic algorithms are known. Crawford (2016) assumes that the recruitment time along any recruitment link is exponentially distributed and thus models RDS as a continuous-time diffusion process. Chen et al. (2016) removes the exponential distribution assumption and extends it to any distribution. Both works use a simulated-annealing-based heuristic to find the most likely configuration.

As a general strategy, for a particular diffusion model, a likelihood function can be derived that measures the probability of a diffusion realization. In this way, the network inference problem can be cast as an optimization problem, in which the researcher seeks the topology that maximizes the likelihood. Unfortunately, the derived likelihood functions are usually intractable for efficient maximization with respect to the graph, and can be computationally prohibitive to evaluate. To address this challenge, approximate solutions have been proposed as an efficient alternative (Gomez-Rodriguez et al., 2010, 2013). For instance, Gomez-Rodriguez et al. (2010), instead of maximizing the likelihood, derived an alternative heuristic formulation by considering only the most likely tree (still an NP-hard problem) rather than all possible propagation trees and showed how a greedy solution can find a near-optimal solution. It enjoys good empirical results when many realizations of the diffusion process can be observed.

In this paper, we consider the challenging instance of network inference where only one realization of the diffusion process is observed. As a motivating empirical example, we study the network reconstruction problem for RDS data and propose VINE (Variational Inference for Network rEconstruction), a computationally efficient variational inference algorithm. Our major contributions are summarized as follows.

Proof of log-submodularity and a variational inference algorithm. We show that under a realistic model of RDS diffusion, the likelihood function is log-submodular. Using variational inference methods, we approximate the submodular function with affine functions and obtain tight upper and lower bounds for the partition function. We then estimate the most probable network configuration, which is the maximizer of the likelihood, as well as the marginal probability of each edge.

Relaxation of constraints. The optimization problem of the RDS likelihood (as shown later) is constrained. First, the observed diffusion results in a directed subgraph and the inferred network must be a supergraph of the diffusion process. Second, for each subject, their degree in the reconstructed subgraph cannot exceed their total network degree. The first constraint is easy to incorporate while the second precludes efficient computation of partition functions of the likelihood (or any linear approximations). We address this challenge by introducing penalty terms in the objective function. This way, the constrained reconstruction problem becomes unconstrained and admits the use of variational methods.

Flexibility for possibly inexact reported degrees. One may not assume that the reported degrees by recruited subjects are exact because subjects may not be able to accurately recall the number of people they know who are members of the target population. We would like to note that the aforementioned relaxation of the second constraint allows for more flexibility of the possible mismatch of the reported degrees from the true ones by introducing an additional term that penalizes the deviation between the reported and true degrees, seeking to preserve the relative accuracy of the reported degrees.

High reconstruction performance and time efficiency using a single realization of RDS diffusion. As shown by our experiments, VINE achieves significantly higher inference performance while running orders of magnitude faster. We should note that the very accurate inference is achieved based on the observation of a single diffusion realization. This is in sharp contrast to previous work that assumes multiple diffusion realizations.

2 NETWORK RECONSTRUCTION FOR RDS DATA

We use the following notational convention throughout this paper. The symbol $\mathbf{1}$ denotes the all-ones column

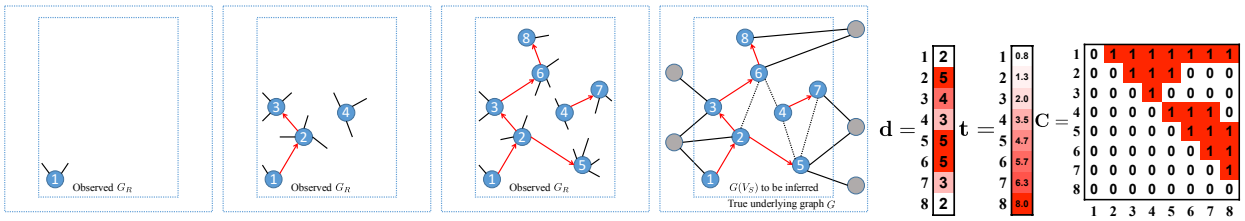

(a) (b) (c) (d) (e) (f) (g)

Figure 1: Example RDS recruitment with unobserved and observed data. Nodes 1 and 4 are seed nodes chosen directly by the researchers; however, only node 1 is recruited at the beginning of the study. Every subject except nodes 3 and 4 is given two coupons, while nodes 3 and 4 are given only one. Figs. 1a to 1c show three snapshots of the RDS process at three different times. Fig. 1a shows the snapshot when the seed node 1 just enters the study due to direct recruitment by the researchers. Node 1 reports that her total degree is 2; thus there are two pendant edges attached to her. Fig. 1b presents the snapshot when the other seed node 4 is directly recruited by the researchers. Before node 4 is recruited, node 1 recruits node 2 and then node 2 recruits node 3. Red arrows denote the recruitment relation. Nodes 2, 3, and 4 report that their total degrees are 5, 4, and 3, respectively; thus there are 5, 4, and 3 pendant edges attached to them, respectively. Fig. 1c illustrates the snapshot at the end of the experiment. Fig. 1d reveals the whole picture of the RDS process, containing the observable part (within the inner rectangle) and the unobservable part (outside the inner rectangle), where the inner rectangle denotes the sample and the outer rectangle denotes the entire population. The dashed lines denote the hidden ties to be inferred within the sample. The nodes outside the inner rectangle are marked in gray and they are the unsampled and thereby unobservable nodes. In Fig. 1e, $\mathbf{d} = (\mathbf{d}_1, \mathbf{d}_2, \mathbf{d}_3, \ldots, \mathbf{d}_n)'$ is the degree vector, where $\mathbf{d}_i$ is the total degree of node i in G. In Fig. 1f, $\mathbf{t} = (\mathbf{t}_1, \mathbf{t}_2, \mathbf{t}_3, \ldots, \mathbf{t}_n)'$ is the recruitment time vector, where $\mathbf{t}_i$ is the recruitment time of node i. In Fig. 1g, $\mathbf{C}$ is the coupon matrix; its (i, j)-entry is 1 if node i has at least one coupon just before the jth recruitment event and is 0 otherwise. The observed data consist of $\mathbf{Y} = (\mathbf{C}, \mathbf{d}, \mathbf{t}, G_R)$.

vector. If f is a real-valued function and that $\mathbf{v}$ is a vector, then $f(\mathbf{v})$ is a vector of the same size as vector $\mathbf{v}$, we denote the i-th entry of $f(\mathbf{v})$ by $f(\mathbf{v})_i$, and $f(\mathbf{v})_i = f(\mathbf{v}_i)$. The transposes of matrix $\mathbf{A}$ and vector $\mathbf{v}$ are written as $\mathbf{A}'$ and $\mathbf{v}'$, respectively.

The objective of the RDS sampling method is to obtain a sample from a population for which random sampling is impossible. The network structure of the underlying inaccessible population is modeled as an undirected simple graph $G = (V, E)$, where each vertex represents an individual and edges represent the intra-population connections. The sample obtained via RDS is denoted by $V_S \subseteq V$. Let $n = |V_S|$ be the number of subjects recruited into the study by the end of the RDS process.

In contrast to random sampling, RDS is a chain-referral process that operates by propagating a diffusion process on the edges of the target social network. Subjects enter the study one at a time. The recruitment (diffusion) process is done either by researchers directly or by other subjects already in the study prior to this new recruitment event. If a subject is recruited into the study by researchers directly, she is called a *seed*. Let $M \subseteq V_S$ be the set of all seed nodes. Note that seed nodes may not necessarily be recruited simultaneously; however, we need at least one seed that enters the study at the initial stage of the experiment in order to initiate the chain-referrals over the underlying network. We label the subjects $i = 1, \ldots, n$ in the time-order they enter the study; node $i \in V_S$ is the i-th subject that enters the study.

When a subject enters the study (either via researchers directly or other subjects already in the study), she will be given several coupons to recruit other members (each recruitment costs one coupon). Each coupon is marked with a unique ID that can be traced back to the recruiter. Subjects are given a reward for being interviewed and recruiting other eligible subjects. The date/time of every subject's recruitment is recorded and every subject reports their total number of acquaintances (their network *degree*). Let $\mathbf{t}_i$ be the recorded recruitment time of subject i and $\mathbf{d}_i$ be the reported degree of subject i in the population (in the graph G). Let the recruitment time and degree vector be $\mathbf{t} = (\mathbf{t}_1, \mathbf{t}_2, \ldots, \mathbf{t}_n)'$ and $\mathbf{d} = (\mathbf{d}_1, \mathbf{d}_2, \ldots, \mathbf{d}_n)'$, respectively.

Once a subject recruits another subject the (directed) link between them will be revealed. The direction simply indicates who recruited whom. Furthermore, any subject who has entered the study with a coupon may not re-enter the study with another coupon, and no participant may enter the study more than once. Thus no subject can recruit others already recruited and thereby already in the study. We can form a directed graph, called the recruitment graph $G_R = (V_R, E_R)$, that has the same vertex set as V_S and reflects the recruitment links; $(i, j) \in E_R$ if and only if subject i directly recruits j. The above requirements will result in a directed recruitment graph G_R being a disjoint union of rooted directed arborescences (a directed graph is a rooted directed arborescence with root r if for every vertex v, there exists a unique directed

path from r to v) (Gordon and McMahon, 1989), where the root corresponds to a seed node. Equivalently, an arborescence is a directed, rooted tree in which all edges point away from the root. We illustrate an example of G_R in Fig. 1d, where the red links form the recruitment graph G_R and there are two disjoint arborescences with roots 1 and 4, respectively; the two roots correspond to the two seed nodes.

The first subject enters the study at time $\mathbf{t}_1$. At some time $t \geq \mathbf{t}_1$, any subject in the study who has at least one coupon (recall that each recruitment costs one coupon and that one cannot recruit any subject without a coupon) and has at least one acquaintance not in the study (i.e., has at least one neighbor in G who is not already recruited) is called a *recruiter* at time t; accordingly, any subject who is not in the study and is connected to at least one recruiter is called a *potential recruitee* or a *susceptible subject* at time t; and the edge between a recruiter and a potential recruitee is said to be *susceptible* at time t. Let $R(i)$ and $I(i)$ be the recruiter set and potential recruitee set just before time $\mathbf{t}_i$, respectively. Similarly, If subject u is a recruiter just before time $\mathbf{t}_i$, then $I_u(i)$ denotes the set of potential recruitees connected to subject u just before time $\mathbf{t}_i$, and if u is a potential recruitee just before time $\mathbf{t}_i$, then $R_u(i)$ denotes the set of recruiters connected to subject u just before time $\mathbf{t}_i$.

In what follows, we model RDS as a continuous-time stochastic process on the edges of a hidden graph. Our goal is to estimate the induced subgraph connecting the sampled vertices G_S. To do this, we construct a flexible model for this process and derive its likelihood, conditional on an underlying graph. The inference problem is to find the graph that maximizes this likelihood, subject to the constraint that the graph must be compatible with the observed degrees in the data. We start with making the following assumptions:

Assumption 1. *Upon entering the study, each subject is given coupons and begins to recruit other members (if any) immediately.*

Assumption 2. *Inter-recruitment times between any recruiter and its potential recruitees are i.i.d. continuous random variables with cumulative distribution function (cdf) $D(t;\theta)$ parametrized by $\theta \in \Theta$.*

In fact, Assumption 2 can be relaxed to the case where inter-recruitment times are independent but not necessarily identically distributed. For simplicity we assume that they are i.i.d.

If W_θ is a random variable with cdf $D(t;\theta)$, we have $D(t;\theta) = \Pr[W_\theta \leq t]$ and let $D_s(t;\theta) = \Pr[W_\theta \leq t | W_\theta > s]$. We write $\rho_s(t;\theta) = \frac{\mathrm{d}D_s(t;\theta)}{\mathrm{d}t}$ for the conditional probability density function (pdf). Let $S_s(t;\theta) = 1 - D_s(t;\theta)$ be the conditional survival function and $H_s(t;\theta) = \frac{\rho_s(t;\theta)}{S_s(t;\theta)}$ be the conditional hazard function. Recall that the set of all subjects in the study is denoted by $V_S = \{1, 2, 3, \ldots, n\} \subseteq V$. The recruitment graph $G_R = (V_R, E_R)$ has the same vertex set as V_S and indicates who recruited whom: $(i, j) \in E_R$ if subject i recruits subject j. Note that subject i can recruit subject j only if there is an edge in the underlying network G that connects i and j. The $n \times n$ coupon matrix $\mathbf{C}$ has a 1 in entry $\mathbf{C}_{ij}$ if subject i has at least one coupon just before the j-th recruitment event $\mathbf{t}_j$, and zero otherwise. In addition, we define another $n \times n$ matrix $\mathbf{A}_R$, which is the adjacency matrix of the undirected version of G_R, obtained by replacing all directed edges with undirected edges.

Assumption 3. *The observed data from an RDS process consists of $\mathbf{Y} = (\mathbf{C}, \mathbf{d}, \mathbf{t}, G_R)$.*

Our goal is to infer the induced subgraph $G(V_S)$, denoted by $G_S = (V_S, E_S)$, which encodes all connections among the subjects in the study. We also use $\mathbf{A}$ to denote the adjacency matrix of G_S and throughout this paper $\mathbf{A}$ and G_S are used interchangeably. Obviously the undirectified version of G_R must be a subgraph of G_S. Thus $\mathbf{A}$ must be greater than or equal to $\mathbf{A}_R$ entrywise; formally,

$$\mathbf{A} \geq \mathbf{A}_R \text{ (entrywise).}$$

This will be a constraint in the optimization problem specified later in Problem 1. Fig. 1 shows an example of an RDS process including its unobserved and observed parts.

Recall that M denotes the set of seeds and let $\tau(u;i) = \mathbf{t}_{i-1} - \mathbf{t}_u$. The likelihood of the recruitment time series is given by

$$\begin{aligned} & L(\mathbf{t}|\mathbf{A}, \theta) \\ =& \prod_{i=1}^{n} \left(\sum_{u \in R(i)} |I_u(i)| H_{\tau(u;i)}(\mathbf{t}_i - \mathbf{t}_u; \theta) \right)^{1\{i \notin M\}} \\ & \times \prod_{j \in R(i)} S_{\tau(j;i)}^{|I_j|}(\mathbf{t}_i - \mathbf{t}_j; \theta) \end{aligned} \tag{1}$$

(The proof of Eq. (1) is presented in Appendix A). The above model was originally derived in (Chen et al., 2016).

We can represent the log-likelihood in a more compact way using linear algebra. Prior to this, we need some notation. Let $\mathbf{m}$ and $\mathbf{u}$ be column vectors of size n such that $\mathbf{m}_i = 1\{i \notin M\}$ and $\mathbf{u}_i$ is the number of pendant edges of subject i (the reported total degree of subject i minus the number of its neighbors in G_S), i.e.,

$$\mathbf{u}_i = \mathbf{d}_i - |\{j \in V_S : (i, j) \in E_S\}|,$$

and let $\mathbf{H}$ and $\mathbf{S}$ be $n \times n$ matrices, defined as $\mathbf{H}_{ui} = H_{\tau(u;i)}(\mathbf{t}_i - \mathbf{t}_u; \theta)$ and $\mathbf{S}_{ji} = \log S_{\tau(j;i)}(\mathbf{t}_i - \mathbf{t}_j; \theta)$. Furthermore, we form matrices $\mathbf{B} = (\mathbf{C} \circ \mathbf{H})$ and $\mathbf{D} = (\mathbf{C} \circ \mathbf{S})$, where $\circ$ denotes the Hadamard (entrywise) product. We let

$$\begin{aligned} \beta &= \log(\mathbf{B}'\mathbf{u} + \mathrm{LowerTri}(\mathbf{AB})' \cdot \mathbf{1}), \\ \delta &= \mathbf{D}'\mathbf{u} + \mathrm{LowerTri}(\mathbf{AD})' \cdot \mathbf{1}, \end{aligned}$$

where the log of a vector is taken entrywise and $\mathrm{LowerTri}(\cdot)$ denotes the lower triangular part (diagonal elements inclusive) of a square matrix. Then the log-likelihood can be written as

$$l(\mathbf{t}|\mathbf{A}, \theta) = \mathbf{m}'\beta + \mathbf{1}'\delta \tag{2}$$

(The proof of Eq. (2) is presented in Appendix B). To adopt a Bayesian approach, we consider maximizing the joint posterior distribution $\Pr(\mathbf{A}, \theta|\mathbf{t}) \propto L(\mathbf{t}|\mathbf{A}, \theta)\pi(\mathbf{A})\phi(\theta)$, where π and ϕ are the prior distribution of $\mathbf{A}$ and θ. The network inference problem of the RDS data is reduced to maximization of $\Pr(\mathbf{A}, \theta|\mathbf{t})$. Our main observation in this paper is that the log-likelihood function is submodular, which opens the possibility of rigorous analysis and variational inference.

If we assume that the reported degrees of subjects are exact, then the vector $\mathbf{u}$ should be set to $\mathbf{d} - \mathbf{A} \cdot \mathbf{1}$ and it must be non-negative entrywise. However, in practice, the reported degree of a subject may be an approximation, but we assume the true degree does not deviate excessively from the reported degree. To be more flexible, we allow $\mathbf{u}$ to be any non-negative integer-valued vector. In this case, the true degree vector will be $\mathbf{d}_{\mathrm{true}} = \mathbf{u} + \mathbf{A} \cdot \mathbf{1}$. We penalize it if $\mathbf{d}_{\mathrm{true}}$ deviates from $\mathbf{d}$ excessively. To be precise, we define the prior distribution $\pi(\mathbf{A})$ as

$$\pi(\mathbf{A}) \propto \exp(-\psi(\max\{\mathbf{u} + \mathbf{A} \cdot \mathbf{1} - \mathbf{d}, \mathbf{0}\})), \tag{3}$$

where $\max$ is conducted entrywise and ψ is a multivariate (n-dimensional) convex function and non-decreasing in each argument whenever this argument is non-negative. We can now formulate our inference problem as an optimization problem.

Problem 1. Given the observed data $\mathbf{Y} = (\mathbf{C}, \mathbf{d}, \mathbf{t}, G_R)$, we seek an $n \times n$ adjacency matrix (symmetric, binary and zero-diagonal) and a parameter value $\theta \in \Theta$ that

$$\begin{array}{rl} \text{maximizes} & L(\mathbf{t}|\mathbf{A}, \theta)\pi(\mathbf{A})\phi(\theta) \\ \text{subject to} & \mathbf{A} \geq \mathbf{A}_R \text{ (entrywise)}. \end{array}$$

Problem 1 can be solved by maximizing the likelihood with respect to θ and $\mathbf{A}$ alternately. We set an initial guess θ_1 for the parameter θ. In the τ-th iteration ($\tau \geq 1$), setting $\theta = \theta_\tau$ in Problem 1, we optimize the objective function over $\mathbf{A}$ (this step is called the $\mathbf{A}$-step), denoting the maximizer by $\mathbf{A}_\tau$; then setting $\mathbf{A} = \mathbf{A}_\tau$ in Problem 1, we optimize the objective function over θ (this step is called the θ-step), denoting the maximizer by $\theta_{\tau+1}$. The interested reader is referred to Algorithm 1 in (Chen et al., 2016). Note that the parameter space Θ is usually a subset of the Euclidean space. The optimization problem given $\mathbf{A}$ in the θ-step can be solved with off-the-shelf solvers. As a result, we focus on the $\mathbf{A}$-step; equivalently, we study how to solve Problem 1 assuming that θ is known.

3 PROPOSED METHOD

We now present a network reconstruction algorithm, based on submodular variational inference, for respondent-driven sampling data. This method is referred to as VINE in this paper. We first introduce the definition of a submodular function (Jegelka et al., 2011; Iyer and Bilmes, 2015).

Definition 1. A pseudo-Boolean function $f : \{0,1\}^p \to \mathbb{R}$ is *submodular* if $\forall \mathbf{x}, \mathbf{y} \in \{0,1\}^p$, we have $f(\mathbf{x}) + f(\mathbf{y}) \geq f(\mathbf{x} \wedge \mathbf{y}) + f(\mathbf{x} \vee \mathbf{y})$, where $\wedge$ and $\vee$ denote entrywise logical conjunction and disjunction, respectively.

We can trivially identify the domain $\{0,1\}^p$ with $2^{[p]}$, the power set of $[p] = \{1, 2, 3, \ldots, p\}$. Thus a pseudo-Boolean function f can also be viewed as a set function $2^{[p]} \to \mathbb{R}$. We will view f from these two perspectives interchangeably throughout this paper. If we view f as a set function, it is submodular if for every subset $X, Y \subseteq [p]$, we have $f(X) + f(Y) \geq f(X \cap Y) + f(X \cup Y)$. An equivalent definition is that f is submodular if for every $X \subseteq Y \subseteq [p]$ and $x \in [p] \setminus Y$, we have $f(X \cup \{x\}) - f(X) \geq f(Y \cup \{x\}) - f(Y)$; this is also known as the "diminishing returns" property because the marginal gain when an element is added to a subset is no less than the marginal gain when it is added to its superset.

A pseudo-Boolean or set function f is *log-submodular* if $\log(f)$ is submodular; it is *modular* if $f(\mathbf{x}) = \sum_{i=1}^p f_i \mathbf{x}_i$ (if viewed as a pseudo-Boolean function) or equivalently $f(X) = \sum_{i \in X} f_i$ (if viewed as a set function), where $f_i \in \mathbb{R}$ is called the weight of the element i. It is *affine* if $f(\mathbf{x}) = s(\mathbf{x}) + c$, where s is modular and c is some fixed real number; similarly, it is *log-affine* if $\log(f)$ is affine.

3.1 RELAXATION OF CONSTRAINTS

The formulation of Problem 1 makes clear that the network reconstruction problem is a constrained optimiza-

tion problem. Recall that we have two constraints. One is that the reconstructed subgraph should contain all edges already revealed by the RDS process. This constraint is natural since if a direct recruitment occurs between two subjects, then they must know each other in the underlying social network. The other constraint is that the degree of the subject in the reconstructed subgraph must be bounded by the degree that this subject reports. In this section, we remove these two constraints and cast it into an unconstrained problem. The first constraint is easy to remove by considering only the edges unrevealed by the RDS process. The final objective function results from replacing the second constraint with a penalty function to allow for some room for the deviation of the degree in the inferred subgraph from the reported degree. After relaxing the two constraints, we turn Problem 1 into an unconstrained problem and make submodular variational inference (to be discussed later in Section 3.3) possible.

Specifically, the first constraint requires some entries of $\mathbf{A}$ to be 1; if the (i,j)-entry of $\mathbf{A}_R$ (denoted by $\mathbf{A}_R^{ij}$) is 1, so is $\mathbf{A}$. Only the rest of the entries of $\mathbf{A}$ can either be 0 or 1 and are the free entries. We collect the free entries in a binary vector

$$\boldsymbol{\alpha} = (\mathbf{A}_{ij} : 1 \le i < j \le n, \mathbf{A}_R^{ij} = 0)$$

and view $L(\mathbf{t}|\mathbf{A},\theta)\pi(\mathbf{A})\phi(\theta)$ as a function of $\boldsymbol{\alpha}$. In fact, there is a one-to-one correspondence between $\mathbf{A}$ and $\boldsymbol{\alpha}$. In this way, we remove the constraint $\mathbf{A} \ge \mathbf{A}_R$. Now we discuss how to relax the second constraint (the degree constraint) to make small deviation from the (usually approximate) reported degree possible.

Representing $\mathbf{u}$ as a binary vector and thereby the objective function as a pseudo-Boolean function. We notice that $L(\mathbf{t}|\mathbf{A},\theta)\pi(\mathbf{A})\phi(\theta)$ is also a function of $\mathbf{u}$; however, $\mathbf{u}$ is an integer-valued vector rather than a binary vector. We consider representing $\mathbf{u}$ as a binary vector and thereby casting $L(\mathbf{t}|\mathbf{A},\theta)\pi(\mathbf{A})\phi(\theta)$ into a pseudo-Boolean function. We observe that $\mathbf{u}$ is bounded entrywise; to be precise, $\forall 1 \le i \le n$, $0 \le \mathbf{u}_i \le u_{\max}$, where $u_{\max} = \max_{1\le i\le n}(\mathbf{d} - \mathbf{A}\cdot\mathbf{1})_i$. We can form an $n \times \lceil \log_2 u_{\max} \rceil$ matrix $\boldsymbol{\mu}$ such that the i-th row of $\boldsymbol{\mu}$ is the binary representation of $\mathbf{u}_i$; formally,

$$\mathbf{u} = \boldsymbol{\mu} \cdot \begin{pmatrix} 2^0 & 2^1 & 2^2 & \dots & 2^{\lceil \log_2 u_{\max} \rceil - 1} \end{pmatrix}'.$$

In this way, we represent $L(\mathbf{t}|\mathbf{A},\theta)\pi(\mathbf{A})\phi(\theta)$ as a pseudo-Boolean function of $\boldsymbol{\alpha}$ and $\boldsymbol{\mu}$. Let $\boldsymbol{\gamma} = (\boldsymbol{\alpha},\boldsymbol{\mu})$ and define $\tilde{L}(\boldsymbol{\gamma}) = L(\mathbf{t}|\mathbf{A},\theta)\pi(\mathbf{A})\phi(\theta)$. Therefore $\tilde{L}$ is a pseudo-Boolean function of $\boldsymbol{\gamma}$, whose dimension is $N = \sum_{1\le i<j\le n} 1_{\{\mathbf{A}_R^{ij}=0\}} + n \times \lceil \log_2 u_{\max} \rceil$. The likelihood function $\tilde{L}(\boldsymbol{\gamma})$ defines a probability measure over $\{0,1\}^N$, $\Pr(\boldsymbol{\gamma}) = \tilde{L}(\boldsymbol{\gamma})/\tilde{Z}$, where $\tilde{Z} = \sum_{\boldsymbol{\gamma}\in\{0,1\}^N} \tilde{L}(\boldsymbol{\gamma})$ is the normalizing constant.

3.2 LOG-SUBMODULARITY OF LIKELIHOOD

Theorem 1 below shows that $\tilde{L}(\boldsymbol{\gamma})$ is log-submodular. We know that a submodular function can be approximated by affine functions from above and below. Due to the log-submodularity of $\tilde{L}(\boldsymbol{\gamma})$, it can be approximated by two log-affine functions from above and below. The partition function of a probability distribution proportional to a log-affine function can be computed in a closed form; therefore this distribution can be computed exactly and we have upper and lower bounds of $\Pr(\boldsymbol{\gamma})$; we can conduct variational inference via the two bounds. We will elaborate on this in Section 3.3.

Theorem 1 (**Proof in Appendix C**). *The function $\tilde{L}(\boldsymbol{\gamma})$ is log-submodular; equivalently, there exists a submodular function $\tilde{F}(\boldsymbol{\gamma})$ such that $\tilde{L}(\boldsymbol{\gamma}) = \exp\tilde{F}(\boldsymbol{\gamma})$ for every $\boldsymbol{\gamma} \in \{0,1\}^N$.*

Normalizing $\tilde{L}(\boldsymbol{\gamma})$ into $L(\boldsymbol{\gamma})$. Ideally, we want a submodular function F to be *normalized*; i.e., $F(\mathbf{0}) = 0$, or equivalently $F(\varnothing) = 0$ if viewed as a set function. Thus we define $F(\boldsymbol{\gamma}) \triangleq \tilde{F}(\boldsymbol{\gamma}) - \tilde{F}(\mathbf{0})$; this way F is a normalized submodular function (it is a submodular function minus some constant). In addition, we define $L(\boldsymbol{\gamma}) = \exp(F(\boldsymbol{\gamma}))$ and we have $L(\boldsymbol{\gamma}) = \exp(\tilde{F}(\boldsymbol{\gamma}) - \tilde{F}(\mathbf{0})) = \exp(-\tilde{F}(\mathbf{0}))\tilde{L}(\boldsymbol{\gamma})$. Note that the probability measure is proportional to $\tilde{L}(\boldsymbol{\gamma}) = L(\mathbf{t}|\mathbf{A},\theta)\pi(\mathbf{A})\phi(\theta)$ (up a constant factor) and that $L(\boldsymbol{\gamma})$ only differs from $\tilde{L}(\boldsymbol{\gamma})$ up to a constant factor. Therefore the probability measure remains proportional to $L(\boldsymbol{\gamma})$, thus $L(\boldsymbol{\gamma})$ is also a likelihood function and defines the same probability measure over $\{0,1\}^N$ as $\tilde{L}(\boldsymbol{\gamma})$ does. As a result, the probability measure can be expressed as $\Pr(\boldsymbol{\gamma}) = \frac{1}{Z}\exp(F(\boldsymbol{\gamma}))$, where $Z = \sum_{\boldsymbol{\gamma}\in\{0,1\}^N}\exp(F(\boldsymbol{\gamma}))$ is the normalizing constant, or the *partition function*.

3.3 VARIATIONAL INFERENCE

Using a variational method lets us consider bounding $F(\boldsymbol{\gamma})$ from above and from below with affine functions. We want to find modular functions s_u and s_l and two real numbers c_u and c_l such that $s_l(\boldsymbol{\gamma}) + c_l \le F(\boldsymbol{\gamma}) \le s_u(\boldsymbol{\gamma}) + c_u$ for all $\boldsymbol{\gamma} \in \{0,1\}^N$. If this holds for all $\boldsymbol{\gamma} \in \{0,1\}^N$, then we have the inequality between log-partition functions: $\sum_{\boldsymbol{\gamma}\in\{0,1\}^N}\exp(s_l(\boldsymbol{\gamma}) + c_l) \le \sum_{\boldsymbol{\gamma}\in\{0,1\}^N}\exp F(\boldsymbol{\gamma}) = Z \le \sum_{\boldsymbol{\gamma}\in\{0,1\}^N}\exp(s_u(\boldsymbol{\gamma}) + c_u)$. We define the partition function of the affine function $s(\boldsymbol{\gamma}) + c$ as $Z(s,c) \triangleq \sum_{\boldsymbol{\gamma}\in\{0,1\}^N}\exp(s(\boldsymbol{\gamma}) + c)$. Using this notation, we have $Z(s_l,c_l) \le Z \le Z(s_u,c_u)$. Note that from this we may also obtain the bounds for the marginal probability for

each element $i \in [N]$. To be precise, if $\boldsymbol{\gamma}$ is sampled from the distribution $\Pr(\boldsymbol{\gamma}) = \exp(F(\boldsymbol{\gamma}))/Z$, then the marginal probability $\Pr(i \in \boldsymbol{\gamma})$ satisfies $\frac{s_l(\{i\})+c_l}{Z(s_u,c_u)} \leq \Pr(i \in \boldsymbol{\gamma}) \leq \frac{s_u(\{i\})+c_u}{Z(s_l,c_l)}$. We may also use $s_u(\boldsymbol{\gamma}) + c_u$ or $s_l(\boldsymbol{\gamma}) + c_l$ as a surrogate for F and make inference via these two affine functions.

Suppose that we already have two affine functions $s_u(\boldsymbol{\gamma})+c_u$ and $s_l(\boldsymbol{\gamma})+c_l$ bounding $F(\boldsymbol{\gamma})$ from above and below. By Lemma 1 in (Djolonga and Krause, 2014), the log-partition function for $s(\boldsymbol{\gamma}) + c$ in the unconstrained case is $\log Z'(s, c) \triangleq \log \sum_{\boldsymbol{\gamma} \in \{0,1\}^N} \exp(s(\boldsymbol{\gamma}) + c) = c + \sum_{i=1}^N \log(1 + \exp s_i)$, where $s_i = s(\{i\})$ is the weight of element i. Thus we have $Z'(s_l, c_l) \leq Z = \sum_{\boldsymbol{\gamma} \in \{0,1\}^N} L(\boldsymbol{\gamma}) = \sum_{\boldsymbol{\gamma} \in \{0,1\}^N} \exp F(\boldsymbol{\gamma}) \leq Z'(s_u, c_u)$.

So our goal is to find the upper- and lower-bound affine functions.

Lower-bound affine function. We define $v_j = \arg\max_{k \in [N] \setminus V_j} \left(F(V_j \cup \{k\}) - F(V_j)\right)$, and $s^g_{v_j} = \max_{k \in [N] \setminus V_j} \left(F(V_j \cup \{k\}) - F(V_j)\right)$, where $V_1 = \varnothing$, $V_j = \{v_1, v_2, \ldots, v_{j-1}\}$, and $1 \leq j \leq N$ (Djolonga and Krause, 2014; Iyer et al., 2013). Then we have the affine function s^g that assigns to $i \in [N]$ a weight of s^g_i. Let $s_l(\boldsymbol{\gamma}) = s^g(\boldsymbol{\gamma})$ and $c_l = 0$.

Proposition 1 (Proof in Appendix D). *The affine function s^g is a lower-bound function of the submodular function F; for all $\boldsymbol{\gamma} \in \{0,1\}^N$, $s^g(\boldsymbol{\gamma}) \leq F(\boldsymbol{\gamma})$.*

Upper-bound affine function. We may find an upper-bound affine function for a submodular function via its supergradients. The set of supergradients of a submodular function F at $\mathbf{x} \in \{0,1\}^N$ (Iyer et al., 2013) is defined as

$$\partial^F(\mathbf{x}) = \{s \text{ is modular : } \forall \mathbf{y} \in \{0,1\}^N, F(\mathbf{y}) \leq F(\mathbf{x}) + s(\mathbf{y}) - s(\mathbf{x})\}.$$

If a modular function s is a supergradient of F at $\mathbf{x}$, then the affine function $s(\boldsymbol{\gamma}) + (F(\mathbf{x}) - s(\mathbf{x}))$ is an upper bound of $F(\boldsymbol{\gamma})$. The corresponding log-partition function is $Z'_{\mathbf{x}}(s) = Z'(s, F(\mathbf{x}) - s(\mathbf{x}))$.

We consider three families of supergradient, which are grow ($\hat{s}_{\mathbf{x}}$), shrink ($\check{s}_{\mathbf{x}}$) and bar ($\bar{s}_{\mathbf{x}}$) supergradients at $\mathbf{x}$ (Iyer et al., 2013; Iyer and Bilmes, 2012; Djolonga and Krause, 2014). Let us view $F(\boldsymbol{\gamma})$ as a set function where $\boldsymbol{\gamma} \subseteq [N]$. We define $\Delta_i F(\boldsymbol{\gamma}) = F(\boldsymbol{\gamma} \cup \{i\}) - F(\boldsymbol{\gamma})$, where $i \in [N]$. These three supergradients are defined as follows. If $j \in \mathbf{x}$, then $\hat{s}_{\mathbf{x}}(\{j\}) = \check{s}_{\mathbf{x}}(\{j\}) = \Delta_j F(\mathbf{x} \setminus \{j\})$ and $\bar{s}_{\mathbf{x}}(\{j\}) = \Delta_j F([N] \setminus \{j\})$ if $j \notin \mathbf{x}$, then $\hat{s}_{\mathbf{x}}(\{j\}) = \Delta_j F(\mathbf{x})$ and $\check{s}_{\mathbf{x}}(\{j\}) = \bar{s}_{\mathbf{x}}(\{j\}) = F(\{j\})$. To make the paper self-contained, we include in the appendix the proof of Proposition 2 showing that they are indeed supergradients.

Algorithm 1 VINE

Input: observed data $\mathbf{Y} = (\mathbf{C}, \mathbf{d}, \mathbf{t}, G_R)$
Output: inferred adjacency matrix $\hat{\mathbf{A}}$

function GETLOWERBOUNDAFFINEFUNCTION
  $V_1 \leftarrow \varnothing$
  for $j \leftarrow 1$ **to** N **do**
    $v_j \leftarrow \arg\max_{k \in [N] \setminus V_j} \left(F(V_j \cup \{k\}) - F(V_j)\right)$
    $s^g_{v_j} \leftarrow \max_{k \in [N] \setminus V_j} \left(F(V_j \cup \{k\}) - F(V_j)\right)$
    $V_{j+1} \leftarrow V_j \cup \{v_j\}$
  end for
  return affine function $s_l(\boldsymbol{\gamma}) = \sum_{j=1}^N s^g_j \boldsymbol{\gamma}_j$
end function

function GETUPPERBOUNDAFFINEFUNCTION
  $m_i \leftarrow \log\left(1 + e^{-\Delta_i F([N] \setminus \{i\})}\right) - \log\left(1 + e^{F(\{i\})}\right)$
  Define $m(\mathbf{x}) = \sum_{i=1}^N m_i \mathbf{x}_i$
  $\mathbf{x} \leftarrow \arg\min_{\mathbf{x}} (F(\mathbf{x}) + m(\mathbf{x}))$
  $S_{\mathbf{x}} = \{\hat{s}_{\mathbf{x}}, \check{s}_{\mathbf{x}}, \bar{s}_{\mathbf{x}}\}$
  $s_u \leftarrow \arg\min_{s \in S_{\mathbf{x}}} Z'_{\mathbf{x}}(s)$
  return affine function $s_u(\boldsymbol{\gamma}) + (F(\mathbf{x}) - s_u(\mathbf{x}))$
end function

function VARIATIONALINFERENCE
  $s \leftarrow$ GETUPPERBOUNDAFFINEFUNCTION() or GETLOWERBOUNDAFFINEFUNCTION()
  Select threshold $\zeta \in [\min_i s^\alpha_i, \max_i s^\alpha_i]$
  $\boldsymbol{\alpha}_i \leftarrow 1_{\{s^\alpha_i \geq \zeta\}}$
  Obtain the inferred adjacency matrix $\hat{\mathbf{A}}$ from $\boldsymbol{\alpha}$
end function

Proposition 2 (Proof in Appendix E). *The modular functions $\hat{s}_{\mathbf{x}}$, $\check{s}_{\mathbf{x}}$ and $\bar{s}_{\mathbf{x}}$ are supergradients of the submodular function F at $\mathbf{x}$.*

Define the modular function

$$m(\{i\}) = \log\left(1 + e^{-\Delta_i F([N] \setminus \{i\})}\right) - \log\left(1 + e^{F(\{i\})}\right).$$

By Lemma 4 in (Djolonga and Krause, 2014), we know that these two optimization problems are equivalent:

$$\min_{\mathbf{x}} \log Z'_{\mathbf{x}}(\bar{s}^{\mathbf{x}}) \equiv \min_{\mathbf{x}} F(\mathbf{x}) + m(\mathbf{x}).$$

The right-hand side is an unconstrained submodular minimization problem, which can be solved efficiently (Jegelka et al., 2011). By solving this problem, we obtain a supergradient $\bar{s}^{\mathbf{x}}$ at $\mathbf{x}$ and thus know its partition function $Z'_{\mathbf{x}}(\bar{s}^{\mathbf{x}})$. Then we compute the partition function of grow and shrink supergradients at $\mathbf{x}$ and let s_u be the one with the smallest partition function. Thus the upper-bound affine function is $s_u(\boldsymbol{\gamma}) + (F(\mathbf{x}) - s_u(\mathbf{x}))$.

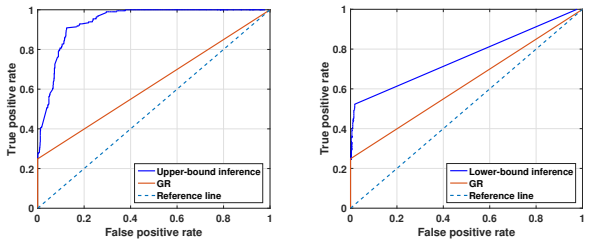

(a) (b)

Figure 2: This figure show an example of the reconstruction results: (a) ROC curves for upper-bound inference and G_R. (b) ROC curves for lower-bound inference and G_R.

When we have an affine approximation for the submodular function, we may make inference via the affine function. Suppose that the affine function is $s(\boldsymbol{\gamma}) + c$, which can be either an upper-bound or lower-bound approximation. Recall that $\boldsymbol{\gamma} = (\boldsymbol{\alpha}, \boldsymbol{\mu})$ and $s(\boldsymbol{\gamma}) = \sum_{i=1}^{N_1} s_i^{\alpha} \boldsymbol{\alpha}_i + \sum_{i=1}^{n} \sum_{j=1}^{N_2} s_{ij}^{\mu} \boldsymbol{\mu}_{ij}$, where $N_1 = \sum_{1 \le i < j \le n} 1_{\{\mathbf{A}_R^{ij} = 0\}}$, $N_2 = \lceil \log_2 u_{\max} \rceil$, and $s_i^{\alpha}, s_{ij}^{\mu} \in \mathbb{R}$.

We can select a threshold $\zeta \in [\min_i s_i^{\alpha}, \max_i s_i^{\alpha}]$ and obtain $\boldsymbol{\alpha}(\zeta)$ by thresholding, $\boldsymbol{\alpha}(\zeta)_i = 1_{\{s_i^{\alpha} \ge \zeta\}}$. Thus we obtain an inferred adjacency matrix $\hat{\mathbf{A}}(\zeta)$ from $\boldsymbol{\alpha}(\zeta)$. The proposed method VINE is presented in Algorithm 1.

4 EXPERIMENT

In this section, we evaluate the proposed variational inference algorithm via experimental results. By varying ζ from $\min_i s_i^{\alpha}$ to $\max_i s_i^{\alpha}$, we obtain a series of inferred adjacency matrices $\hat{\mathbf{A}}(\zeta)$. Suppose that the true adjacency matrix of G_S is $\mathbf{A}$. The reconstruction performance of an inferred adjacency matrix $\hat{\mathbf{A}}$ is measured by the true positive rate (TPR) and the false positive rate (FPR), which are defined as $\mathrm{TPR}(\hat{\mathbf{A}}, \mathbf{A}) = \binom{n}{2}^{-1} \sum_{i<j} 1\{\hat{\mathbf{A}}_{ij} = 1 \text{ and } \mathbf{A}_{ij} = 1\}$ and $\mathrm{FPR}(\hat{\mathbf{A}}, \mathbf{A}) = \binom{n}{2}^{-1} \sum_{i<j} 1\{\hat{\mathbf{A}}_{ij} = 1 \text{ and } \mathbf{A}_{ij} = 0\}$, where n is the number of subjects. We plot the TPR and FPR of each $\hat{\mathbf{A}}(\zeta)$ on the ROC plane and obtain the ROC curve. Figs. 2a and 2b show an example of the reconstruction result. In this example, we simulated an RDS process over a real-world network, the Project 90 graph that represents the community structure of heterosexuals at high risk for HIV infection (Woodhouse et al., 1994), with inter-recruitment time distribution $\mathrm{Exp}(1)$ (exponential distribution with rate 1). In the simulation, we choose $n = |V_S| = 50$, and a single seed subject at the initial stage; each subject is given 3 coupons; 1176 missing edges are to be inferred. In practice, the sample size n is usually fixed in advance (according to researchers' study plan). In Fig. 2a, the blue ROC curve corresponds to the upper-bound inference. We choose ψ to be the L^2 norm. The red curve is a baseline reconstruction given by estimating G_S by G_R. Since G_R must be a subgraph of G_S, the FPR of G_R is zero. The red curve is obtained by connecting the point of the TPR of G_R on the vertical axis and the point $(1, 1)$. The performance is quantified by the area of the region under the ROC curve (note that larger is better). In this example, the area of the region under the blue curve is 0.92 and that of the red curve is 0.64. The region under the blue curve is 47% greater than that of the red curve. With the best thresholding, the algorithm can achieve a TPR of 90% while the FPR is only 10%. In Fig. 2b, the blue curve is the ROC curve of the lower-bound inference. We choose ψ to be the L^2 norm. The red curve is a baseline given by G_R. The area under the blue curve is 0.74, which is 18% greater than that of the red curve. Since the lower-bound approximation is obtained from the greedy algorithm while the upper-bound approximation is the solution to an optimization problem, we focus on the upper-bound inference.

4.1 EXPERIMENTS ON FACEBOOK NETWORK

Recall that in Eq. (3), ψ can be any non-decreasing convex function. We may let $\psi(\cdot) = \omega \|\cdot\|_p$ be ω times the L^p norm ($\omega \ge 0$, $1 \le p \le \infty$). We now study the influence of different choices of ψ.

Influence of p. First we fix $\omega = 1$ and vary p from 1 to 5. We simulated 100 RDS processes over the Facebook network (McAuley and Leskovec, 2012). For each p, we measure the area under the ROC curve of the upper-bound inference for each RDS data and illustrate their distribution with a Tukey boxplot, shown in Fig. 3a. We also record the advantage of the area under the ROC curve of the upper-bound inference over that of G_R; boxplots are given in Fig. 3b. We observe that the variational inference algorithm achieves remarkably high accuracy when $p = 2, 3, 4, 5$.

Influence of ω. We let ψ be $\omega \|\cdot\|_2$ and vary ω from 0.01 to 100. 100 RDS processes are simulated over the Facebook network. For each ω, we measure the area under the ROC curve of the upper-bound inference for each RDS data and illustrate their distribution with a Tukey boxplot. The result is presented in Fig. 3c. In addition, we also record the advantage of the area under the ROC curve of the upper-bound inference over that of G_R. Accordingly, their boxplots are presented in Fig. 3d. From Figs. 3c and 3d, we can observe that the variational infer-

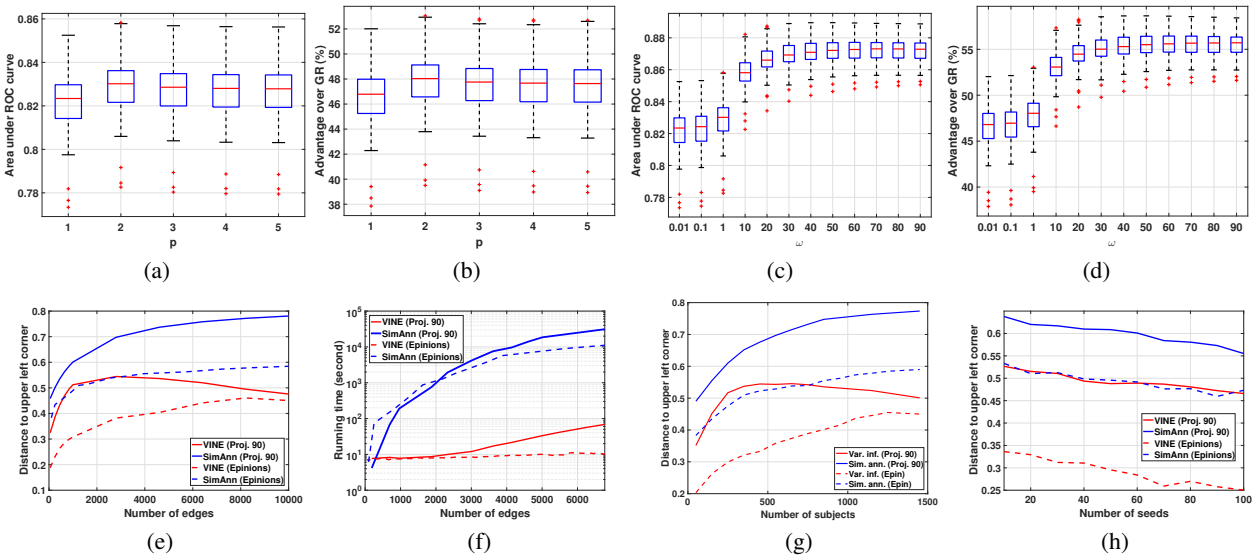

Figure 3: (a) The area under the ROC curve of the upper-bound inference, when ψ is L^p norm and p varies from 1 to 5. (b) Improvement of upper-bound inference over G_R in terms of the area under the ROC curve, as a function of p. (c) Area under the ROC curve for upper-bound inference, when we let ψ be $\omega \|\cdot\|_2$ and ω varies from 0.01 to 100. (d) Improvement of upper-bound inference over G_R in terms of the area under the ROC curve, when we let ψ be $\omega \|\cdot\|_2$ and ω varies from 0.01 to 100. (e) Distance to the upper left corner (the smaller, the better) versus the number of edges in G_S. (f) Running time (in seconds) versus the number of edges in G_S. (g) Distance to the upper left corner versus the number of subjects in the sample (the number of nodes in G_S). (h) Distance to the upper left corner (the smaller, the better) versus the number of seeds.

ence algorithm achieves higher accuracy as ω increases from 0.01 to 10 and that the increase of ω from 10 to 100 leads to lower accuracy of the variational inference.

4.2 EXPERIMENTS ON LARGE PROJECT 90 AND EPINION NETWORKS

We compare VINE with the simulated-annealing-based method proposed in (Chen et al., 2016) (referred to as SIMANN). Since SIMANN only gives a single point on the ROC plane rather than a curve, thus the reconstruction performance in this set of experiments is quantified by the distance from the output point to the upper left corner, $[(1 - \text{TPR})^2 + \text{FPR}^2]^{1/2}$. The algorithm with smaller distance is considered to attain better performance. We apply both methods to the large Project 90 network (Woodhouse et al., 1994) and the Epinions social network (Richardson et al., 2003). The Epinions network characterizes the trust relationships between users of a general consumer review site Epinions.com.

Fig. 3e shows the distance to the upper left corner versus the number of edges in G_S, where the ζ value is chosen to minimize the distance of the VINE ROC curve datapoint to the upper-left corner $(0, 1)$; we vary from tens of edges to 10000 edges. We generate many RDS processes with different sample sizes and sort them according to the number of edges in G_S and see the reconstruction performance on these datasets. In this way, we plot how the reconstruction performance varies with the number of edges in G_S. Fig. 3g presents the distance to the upper left corner versus the number of subjects in the sample (the number of nodes in G_S). VINE outperforms SIMANN significantly on both datasets. Fig. 3f presents the running time (in seconds) versus of the number of edges in G_S. SIMANN was implemented in C++ while VINE was written in the Julia language and can be implemented as a parallelized version. VINE runs three orders of magnitude faster than SIMANN when there are more edges in G_S and VINE is more scalable for large graphs.

Fig. 3h shows the distance to the upper left corner versus the number of seeds. We vary the number of seeds from 10 to 100, while fixing the sample size. Both algorithms achieve better reconstruction performance with more seeds and that under the same number of seeds, VINE attains a remarkably better performance than SIMANN.

Acknowledgements

LC and AK were supported by DARPA Young Faculty Award (D16AP00046). FWC was funded by NIH grant 1DP2 OD022614-01. LC would like to thank Zheng Wei.

References

Animashree Anandkumar, Avinatan Hassidim, and Jonathan Kelner. Topology discovery of sparse random graphs with few participants. *ACM SIGMETRICS Performance Evaluation Review*, 39(1):253–264, 2011.

Stephen Boyd and Lieven Vandenberghe. *Convex optimization*. Cambridge university press, 2004.

Lin Chen, Forrest W Crawford, and Amin Karbasi. Seeing the unseen network: Inferring hidden social ties from respondent-driven sampling. In *AAAI*, pages 1174–1180, 2016.

Forrest W Crawford. The graphical structure of respondent-driven sampling. *Sociological Methodology*, 46(1):187–211, 2016.

H. Daneshmand, M. Gomez-Rodriguez, L. Song, and B. Schölkopf. Estimating diffusion network structures: Recovery conditions, sample complexity & soft-thresholding algorithm. In *ICML*, 2014.

Josip Djolonga and Andreas Krause. From map to marginals: Variational inference in bayesian submodular models. In *NIPS*, December 2014.

Mehrdad Farajtabar, Manuel Gomez Rodriguez, Mohammad Zamani, Nan Du, Hongyuan Zha, and Le Song. Back to the past: Source identification in diffusion networks from partially observed cascades. In *AISTATS*, pages 232–240, 2015.

Qi Gao, Fabian Abel, Geert-Jan Houben, and Yong Yu. A comparative study of users' microblogging behavior on sina weibo and twitter. In *UMAP*, pages 88–101. Springer, 2012.

M. Gomez-Rodriguez, J. Leskovec, and B. Schölkopf. Structure and dynamics of information pathways in on-line media. In *WSDM*, 2013.

Manuel Gomez-Rodriguez, Jure Leskovec, and Andreas Krause. Inferring networks of diffusion and influence. In *SIGKDD*, pages 1019–1028. ACM, 2010.

Manuel Gomez-Rodriguez, Jure Leskovec, David Balduzzi, and Bernhard Schölkopf. Uncovering the structure and temporal dynamics of information propagation. *Network Science*, 2(01):26–65, 2014.

Gary Gordon and Elizabeth McMahon. A greedoid polynomial which distinguishes rooted arborescences. *Proceedings of the AMS*, 107(2):287–298, 1989.

Steve Hanneke and Eric P Xing. Network completion and survey sampling. In *AISTATS*, pages 209–215, 2009.

Douglas D Heckathorn. Respondent-driven sampling: a new approach to the study of hidden populations. *Social Problems*, 44(2):174–199, 1997.

Rishabh Iyer and Jeff Bilmes. Polyhedral aspects of submodularity, convexity and concavity. *arXiv preprint arXiv:1506.07329*, 2015.

Rishabh Iyer and Jeff A Bilmes. Submodular-Bregman and the Lovász-Bregman divergences with applications. In *NIPS*, pages 2933–2941, 2012.

Rishabh Iyer, Stefanie Jegelka, and Jeff A. Bilmes. Fast semidifferential-based submodular function optimization. In *ICML*, 2013.

Stefanie Jegelka, Hui Lin, and Jeff A Bilmes. On fast approximate submodular minimization. In *NIPS*, pages 460–468, 2011.

Myunghwan Kim and Jure Leskovec. The network completion problem: Inferring missing nodes and edges in networks. In *SDM*, volume 11, pages 47–58, 2011.

Mark A Kramer, Uri T Eden, Sydney S Cash, and Eric D Kolaczyk. Network inference with confidence from multivariate time series. *Physical Review E*, 79(6): 061916, 2009.

David Liben-Nowell and Jon Kleinberg. The link-prediction problem for social networks. *Journal of the American society for information science and technology*, 58(7):1019–1031, 2007.

Scott Linderman and Ryan Adams. Discovering latent network structure in point process data. In *ICML*, pages 1413–1421, 2014.

Julian J McAuley and Jure Leskovec. Learning to discover social circles in ego networks. In *NIPS*, pages 548–56, 2012.

Matthew Richardson, Rakesh Agrawal, and Pedro Domingos. Trust management for the semantic web. In *ISWC*, pages 351–368. Springer, 2003.

Srinivas Gorur Shandilya and Marc Timme. Inferring network topology from complex dynamics. *New Journal of Physics*, 13(1):013004, 2011.

Donald E Woodhouse, Richard B Rothenberg, John J Potterat, William W Darrow, et al. Mapping a social network of heterosexuals at high risk for HIV infection. *AIDS*, 8(9):1331–1336, 1994.